Turbulent Thermal Convection with an Obstructed Sidewall

Ke-Qing Xia* and Siu-Lung Lui
Department of Physics, The Chinese University of Hong Kong, Shatin, New Territories, Hong Kong
(Received 7 July 1997)

We present an experimental study of turbulent convection in a cell with staggered fingers on its sidewall using water as the convecting fluid. Our measurements reveal that $\mathrm{Nu} \sim \mathrm{Ra}^{-0.27}$, and that the temperature probability density function (PDF) at the cell center is a double-peaked function which can be fitted by the superposition of two Gaussians. Moreover, it is found that the size of the local temperature fluctuations scales with Ra and that the scaled PDFs for different Ra have an invariant form. Visualization studies show that the mean flow pattern in the cell is a twisted asymmetric four-roll circulation, which helped to explain the observed PDF. [S0031-9007(97)04841-2]

PACS numbers: 47.27.Te, 44.25.+f

The discovery of a new scaling state [1–3], called hard turbulence, in Rayleigh-Bénard (RB) convection has stimulated considerable recent interest in the study of convective turbulence [4]. It is now generally accepted that this hard turbulence state has three "hallmarks," namely, (i) a "nonclassical" scaling dependence of the dimensionless heat flux Nu on the Rayleigh number, i.e., $\mathrm{Nu} \sim \mathrm{Ra}^{2/7}$; (ii) the exponential functional form of the probability density function (PDF) for the temperature fluctuations at the center of the convection cell; and (iii) the existence of a coherent large scale circulation. It is also believed that the large-scale circulation (LSC) plays an important role in determining the heat flux in hard turbulent state [5,6]. In fact, one theoretical model aimed at explaining the observed heat flux scaling and temperature statistics takes into account explicitly the role played by the LSC in heat transport [7]. Among the many experimental investigations of the hard turbulence state, several are specifically devoted to the study of the large-scale flow such as visualization studies [8], and artificially shearing the thermal boundary layer which mimics the effect of LSC [9]. There is also a recent study [10] in a cell with rough horizontal plates aimed at increasing the emission of thermal plumes from the boundary layers, the plumes are believed to transport heat across the cell in competition with the LSC. Therefore, one would ask what will happen to the scaling of the heat flux, and to the hard turbulence state, if the large-scale circulation were suppressed or strongly perturbed. By modifying the boundary conditions of the convection cell, one can either suppress the LSC or modify its flow pattern. Thus, studying the effect of the boundary modifications on the heat transport, temperature statistics, and other relevant quantities will help us to pinpoint the role played by the LSC in turbulent convection.

In this Letter, we present results from a convection experiment which was specifically designed to address the above question [11]. The experiment used a convection cell with three staggered layers of "fingers" on its sidewall to suppress the large-scale flow. The inset of Fig. 1 shows a schematic drawing of the convection cell, which is a vertical cylinder with its inner diameter and height being 19 and 19.6 cm, respectively (the aspect ratio is thus 1). The upper and lower plates were made of copper and their surfaces were plated with gold. The sidewall of the cell was a cylindrical tube made of transparent Plexiglas. The rectangular shaped Plexiglas fingers were 2 mm in thickness and 3 cm in length. Their width was 1 cm and they were placed in equal distance around the sidewall with a spacing of 1 cm. The length of the fingers was chosen according to the width of the LSC which is a band of a few centimeters wide as measured in a recent light scattering experiment [12]. The fingers in the top layer were directly above those in the bottom layer, while the ones in the middle layer were above (below) the "opening" positions of the bottom (top) layer. Thus these staggered fingers will block fluids from directly passing through.

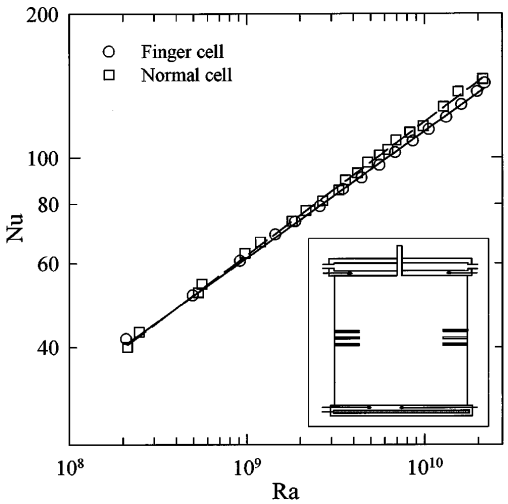

FIG. 1. Nu as a function of Ra measured from the finger cell and the normal cell, respectively. The solid line is a power-law fit to the circles: $\mathrm{Nu} = 0.24\mathrm{Ra}^{0.266}$; and the dashed line is a fit to the squares: $\mathrm{Nu} = 0.19\mathrm{Ra}^{0.280}$. The inset is a sketch of the convection cell used in the experiment, which had three layers of staggered fingers on its sidewall.

 0031-9007/97/79(25)/5006(4)$10.00

The middle layer was placed at equal distance of 1.5 cm from the other two, and at the mid-height of the cell. The temperature of the upper plate was regulated by passing cold water through a cooling chamber fitted on the top of the plate. The lower plate was heated uniformly at a constant rate with an imbedded film heater. The temperature difference Δ between the two plates was measured by four thermistors imbedded inside the plates. The two thermistors at top plate were at one third radius from the edge at opposite positions. While the two at the bottom plate were placed at, respectively, the center and the half-radius position. It was found that the measured relative temperature difference between the two thermistors in the same plate were less than 1% for both plates at all Ra. This indicates that the temperature was uniform across the horizontal plates. The control parameter in the experiment is the Rayleigh number $\mathrm{Ra} = \alpha g L^3 \Delta / \nu\kappa$, with g being the gravitational acceleration, L the height of the cell, and α, ν, and κ being, respectively, the thermal expansion coefficient, the kinematic viscosity, and the thermal diffusivity of water, which was the convecting fluid. During our experiment, the average temperature of water in the convection cell was kept near room temperature and only the temperature difference across the cell was changed. In this way, the variation of the Prandtl number $\mathrm{Pr} = \nu/\kappa$ was kept at minimum ($\mathrm{Pr} \simeq 7$). We present below results from measurements of the temperature field in the convection cell with fingers. For comparison, we also measured corresponding quantities in a "normal" cell which has a smooth sidewall but is otherwise identical to the finger cell.

Figure 1 shows the measured Nu vs Ra in a log-log scale where circles represent data from the finger cell, and squares those from the normal cell. The measurement was made over a range of Ra which spans from 2×10^8 to 2×10^{10}. It is seen from the figure that Nu has essentially the same scaling with Ra with or without the fingers. The solid and dashed lines are power-law fits to the respective data, finger: $\mathrm{Nu} = (0.25 \pm 0.06)\mathrm{Ra}^{0.266\pm0.003}$; normal: $\mathrm{Nu} = (0.19 \pm 0.02)\mathrm{Ra}^{0.280\pm0.003}$. These exponents are in line with the values $0.275 \sim 0.280$ obtained by others [9,13,14] in water. Thus, the Nu scaling in the finger cell can be taken as still within the "2/7" regime.

We now examine the local statistical properties of the temperature field in the convection cell. The local temperature was measured using a thermistor 300 μm in size with a time constant of 10 ms [15]. The thermistor was mounted on a stainless steel tube of 1 mm in diameter which was inserted into the cell through its filling stem. The thermistor served as one arm of an ac Wheatstone bridge which was driven by a sinusoidal source of 1 kHz. The output of the bridge was first fed to a lock-in amplifier and then digitized by a dynamic signal analyzer (HP 35670A) at a sampling rate of 250 Hz. For each measurement, a 6-h time series was recorded first and from it the histogram was computed by the signal analyzer. It was found that all histograms, or probability density function (PDF), measured in the *normal* cell for Ra from 2×10^8 to 2×10^{10} have exponential functional form, and the scaled histograms are invariant. Figure 2(a) shows four typical PDFs measured at the center of the normal cell. The vertical axis is the normalized histogram (relative frequency of observing a particular temperature T) in log scale and the horizontal axis is the scaled temperature fluctuation $(T - \langle T\rangle)/\sigma$. The standard deviation (the size of local temperature fluctuation), $\sigma = \langle (T - \langle T\rangle)^2\rangle^{1/2}$, of the PDFs has a power-law dependence on Ra as is shown in Fig. 2(b) (denoted as σ_N for normal cell), where it is normalized by the corresponding temperature difference Δ between the horizontal plates. The dashed line in the figure is a fit of $\sigma/\Delta = (0.29 \pm 0.01)\mathrm{Ra}^{-0.145\pm0.004}$, which is in excellent agreement with that found in the helium gas experiment [2]. Next, we show in Fig. 3 a typical histogram measured at the center of the *finger* cell. It is seen that the PDF has changed dramatically into a double-peaked function. We fitted the PDF by two separate Gaussian functions to the two peaks, respectively. The two solid curves in Fig. 3 represent the fitting function: $A_x \exp[-(T - T_x)^2/2\sigma_x^2]$, where A_x is an amplitude, and x denotes either L (left peak) or R (right peak). As will be explained below, these two peaks are due to the up and down currents from the bottom and top plates, respectively. It is found that all measured PDFs at different Ra have the double-peaked form and can be well fitted with Gaussian functions, while

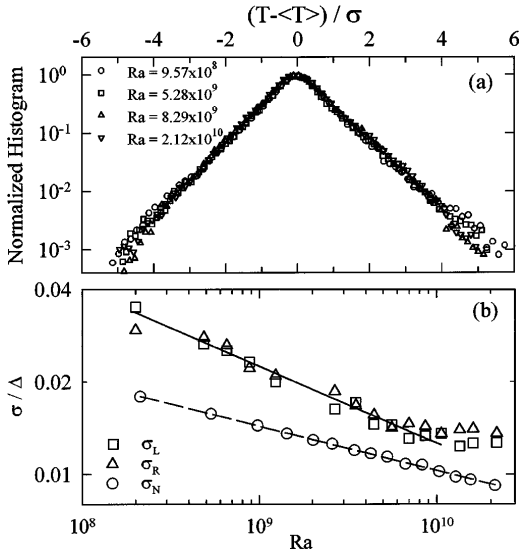

FIG. 2. (a) Scaled PDF from the normal cell measured at four different Ra; (b) Standard deviations of the local temperature fluctuations vs Ra as measured in the normal cell (σ_N) and the finger cell (σ_L and σ_R). The solid and dashed lines represent power-law fits of $\sigma_{L,R}/\Delta = (3.3 \pm 0.1)\mathrm{Ra}^{-0.24\pm0.01}$ and $\sigma_N/\Delta = (0.29 \pm 0.01)\mathrm{Ra}^{-0.145\pm0.002}$, respectively.

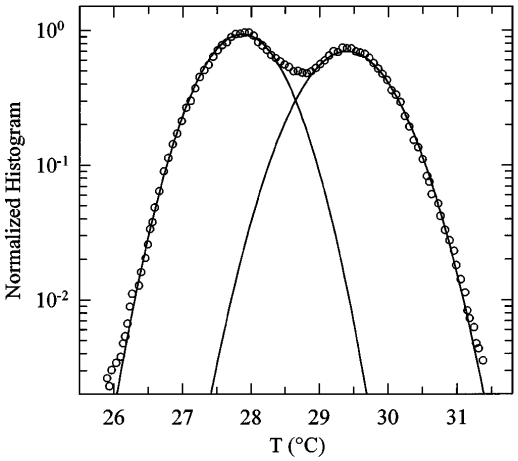

FIG. 3. PDF measured at the center of the finger cell at Ra = 6.99×10^9. The two solid curves represent separate Gaussian function fits to the left and the right peaks, respectively (see text).

the relative heights of the two peaks do not have fixed ratios. The Ra dependence of the fitted σ_L and σ_R are shown in Fig. 2(b). It is seen that temperature fluctuations in the finger cell are greatly enhanced throughout the entire range of Ra as compared to the normal cell, there is also no systematic difference between σ_L and σ_R, though fluctuations of the right (hotter) peak are generally larger than those of the left (cooler) peak. Note that the fluctuations in the finger cell decay faster with increasing Ra as compared to those in the normal cell, and for Ra $> 1 \times 10^{10}$ there is an apparent level-off for both σ_L and σ_R (we also noticed the corresponding PDFs show slight deviations from pure Gaussians). The solid line in Fig. 2(b) represents a power-law fit to the combined data set of σ_L and σ_R for Ra $\leq 1 \times 10^{10}$, which gave $\sigma_{L,R}/\Delta = (3.3 \pm 0.1)\mathrm{Ra}^{-0.24\pm0.01}$. When the fitted values of σ_x are used to scale the corresponding peaks of the measured histograms, it is found that they all collapse onto a single curve. We show in Fig. 4 a few typical scaled PDFs from the finger cell, where the left and the right peaks were plotted separately. It is seen that, like the exponential PDFs in the normal cell, the Gaussian PDFs in the finger cell also have an invariant form which is independent of Ra. Indeed, when flipped about the vertical axis, the two data sets in Figs. 4(a) and 4(b) will fold over exactly on top of each other. This is in contrast to the Gaussian PDFs observed in the soft-turbulence regime in a normal cell, where no universal behavior and power law were observed [3,9]. Combining the Nu and PDF results, we conclude that the turbulent fluid motion in the finger cell at the present range of Ra is in a scaling state, just like the hard-turbulence state in the normal cell. It should be pointed out, however, that Gaussian-like PDFs in the "2/7" scaling regime have also been observed at the center of large aspect ratio cells ($A \geq 6$) in experiment [16] and in numerical simulations

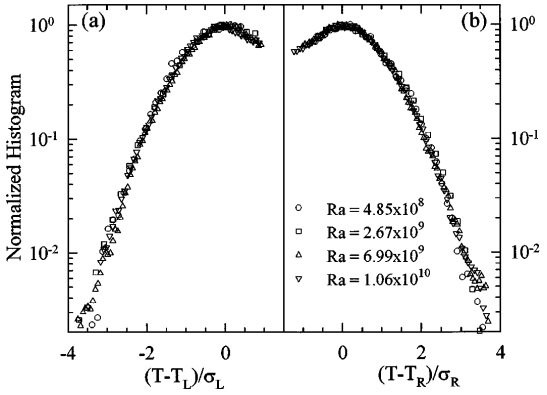

FIG. 4. Scaled PDFs from the finger cell measured at four different Ra: (a) the left peaks, (b) the right peaks.

[17]. As flow patterns in the convection cell have a strong dependence on its aspect ratio, these results suggest that the functional form of the temperature PDF is influenced by flow patterns.

To further characterize the state of motion in the finger cell, we conducted a visualization experiment. Because of the cylindrical shape of our cell, it is difficult to make good shadowgraphs. Instead, we shed a vertical laser sheet of 2 mm in thickness through the sidewall of the cell, passing through its central axis. The fluid was then seeded with 45 μm diameter latex spheres to visualize the flow. While the contrast between the streaklines of the particles and the background fluid was not sufficient to render print-quality photographic images, visual observations reveal that the large-scale flow has changed into a distorted four-roll circulation. We illustrate in Fig. 5 the observed mean flow patterns, where it is seen that the large-scale circulation is not fully "suppressed" but merely distorted in the sense that the circulation still spans the height of the cell and the horizontal "winds" still sweep across the conducting plates. It is also seen that the LSC stagnates near the top and bottom plates and branches into an asymmetric four-roll circulation. This situation is different from the experiment described in Ref. [11], where it was reported that the vertical screens at the conducting plates not only suppressed the LSC near the boundary layers, but also

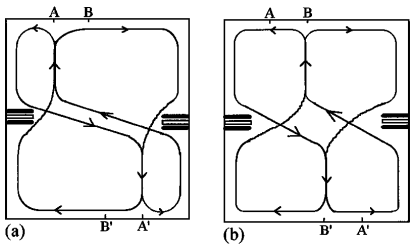

FIG. 5. Schematic drawing of the mean circulation pattern in the finger cell, (a) and (b), showing the stagnation points at their extreme positions.

destroyed its coherence. We also observed that the two stagnation points are oscillating in phase along opposite horizontal directions as illustrated in Figs. 5(a) and 5(b), where the stagnation points are shown in their extreme positions, respectively. The oscillation is not quite regular in that the two stagnation points sometime reverse their direction before reaching B and B', so they spend more time near A and A'. The points of A and A' are located at roughly half-way between the sidewall and the center axis of the cell, while B and B' are visibly off the center axis (B to the left and B' to the right) so the four-roll pattern is never symmetric. The oscillation period fluctuates somewhat and was estimated to be around 15 sec at $\mathrm{Ra} = 6 \times 10^9$, which is consistent with the measured time series at the same Ra. Because of this oscillation, the thermistor probe at cell center "feels" the up (hot) and down (cold) currents alternatively, which explains the double-peaked PDF and justified our earlier assertion that the peak positions of the PDF correspond to the mean temperature of the up and down streams at cell center. We also observed that, because of the particular flow pattern, more plumes are brought to the central part of the cell by the circulating currents. Whereas in the normal cell, the LSC sweeps and carries the plumes from one plate to the other along the perimeter of the cell, so a relatively fewer number of plumes are able to "escape" and thereby travel through the center region of the cell. This is also evident when comparing the time series measured at the center of the two cells, where more intermittent spikes with larger amplitudes are observed in the time series for the finger cell. To further investigate the role played by the thermal plumes in determining the functional form of the temperature PDF, we measured temperature fluctuations near the centers of the two upper circulating rolls. We found that the corresponding PDFs there indeed have clear exponential tails with rounded peaks. Because of the particular flow pattern existing in the finger cell, the centers of the four rolls are outside the path of the LSC and a smaller number of thermal plumes will pass through these regions than at the cell center. Thus the measurements at the centers of the circulating rolls provide strong evidence that thermal plumes are responsible for the observed Gaussian-like temperature PDF. This is also consistent with the observations made by Solomon and Gollub [9] that the coherence of plumes determines the form of PDF.

To summarize, our experiment shows that the $2/7$ scaling of the Nu and the exponential temperature PDF are not necessarily concomitant features in high Rayleigh number turbulent convection even for an aspect-ratio-one cell, and different mechanisms are responsible for these characteristics of hard convective turbulence. Our results also show that different flow patterns in the convection cell may change temperature statistics but not the heat flux scaling. Moreover, the turbulence regime found in a cell with staggered fingers on its sidewall is a scaling state with a universal Gaussian-like temperature PDF at cell center, and the enhanced temperature fluctuations show a different scaling from those in a normal cell. These results will put new (or remove old) constraints in future theoretical models of hard-turbulent convection.

Support of this work by the Hong Kong Research Grants Council under Grant No. CUHK 319/96P is gratefully acknowledged.

*Electronic address: kxia@phy.cuhk.edu.hk

[1] F. Heslot, B. Castaing, and A. Libchaber, Phys. Rev. A **36**, 5870 (1987).
[2] B. Castaing, G. Gunaratne, F. Heslot, L. P. Kadanoff, A. Libchaber, S. Thomae, X.-Z. Wu, S. Zaleski, and G. Zanetti, J. Fluid Mech. **204**, 1 (1989).
[3] M. Sano, X.-Z. Wu, and A. Libchaber, Phys. Rev. A **40**, 6421 (1989).
[4] See the review by E. D. Siggia, Annu. Rev. Fluid Mech. **26**, 137 (1994), and references therein.
[5] A. Belmonte, A. Tilgner, and A. Libchaber, Phys. Rev. E **50**, 269 (1994).
[6] E. Villermaux, Phys. Rev. Lett. **75**, 4618 (1995).
[7] B. I. Shraiman and E. D. Siggia, Phys. Rev. A **42**, 3650 (1990).
[8] G. Zocchi, E. Moses, and A. Libchaber, Physica (Amsterdam) **166A**, 387 (1990).
[9] T. H. Solomon and J. P. Gollub, Phys. Rev. Lett. **64**, 2382 (1990); Phys. Rev. A **43**, 6683 (1991).
[10] Y. Shen, P. Tong, and K.-Q. Xia, Phys. Rev. Lett. **76**, 908 (1996).
[11] After commencing our experiment, we learned the study by S. Ciliberto, S. Cioni, and C. Laroche [Phys. Rev. E **54**, R5901 (1996)]. In their experiment, vertical screens were placed on the conducting plates.
[12] Y.-B. Xin, K.-Q. Xia, and P. Tong, Phys. Rev. Lett. **77**, 1266 (1996).
[13] T. Y. Chu and R. J. Goldstein, J. Fluid. Mech. **60**, 141 (1973).
[14] F. Chillá, S. Ciliberto, C. Innocenti, and E. Pampaloni, Nuovo Cimento D **15**, 1229 (1993).
[15] Model AB6E3-B10KA103J, Thermometrics Inc.
[16] X.-Z. Wu and A. Libchaber, Phys. Rev. A **45**, 842 (1992).
[17] S. L. Christie and J. A. Domaradzki, Phys. Fluids A **5**, 412 (1993); **6**, 1848 (1994).